International Journal of Pharmacology

Int. J. Pharmacol. **2026**; 22(6): 50778
https://doi.org/10.31083/IJP50778

Research Article

Betulonic Acid Inhibits HBV Replication via Modulating ERK1/2-HNF4α Axis

Qianqian Xu[1,2,†], Sien Ma[1,2,†], Yan Pan[2], Shumin Li[2], Yuting Zhu[2], Lulu Wang[3], Jiawei Chen[3], Yarong Liu[1], Mengmeng Deng[3,*], Bao Zhao[1,2,*]

[1]School of Pharmacy, Center for Xin'an Medicine and Modernization of Traditional Chinese Medicine of IHM, Anhui University of Chinese Medicine, 230012 Hefei, Anhui, China
[2]Institute of Health and Medicine, Hefei Comprehensive National Science Center, 230000 Hefei, Anhui, China
[3]Department of Clinical Laboratory, The First Affiliated Hospital of Bengbu Medical University, 233004 Bengbu, Anhui, China
*Correspondence: mmdeng@mail.ustc.edu.cn (Mengmeng Deng); zhaobao@ihm.ac.cn (Bao Zhao)
†These authors contributed equally.
Academic Editor: Mehmet Ozaslan
Submitted: 6 February 2026 Revised: 27 April 2026 Accepted: 14 May 2026 Published: 21 October 2026

Abstract

Background: Chronic hepatitis B virus (HBV) infection continues to pose a significant global public health burden. Existing therapies achieve functional cures at limited rates and are complicated by problems including drug resistance and cumulative toxicity. Betulonic acid (Bet) is known for its anti-inflammatory, antibacterial, and antitumor activities. However, whether its antimicrobial effects extend to HBV infection remains unclear. Consequently, this study investigates the antiviral effects of Bet both *in vitro* and *in vivo*. **Methods:** Bet effect on HBV replication and transcription was first investigated using Enzyme-Linked Immunosorbent Assay (ELISA) and real-time quantitative reverse transcription (RT-qPCR). Western blot and RNA-seq analyses were performed to elucidate the antiviral mechanism. Finally, animal experiments were conducted to assess the *in vivo* anti-HBV effect of Bet. **Results:** *In vitro* experiments demonstrated that Bet significantly inhibited secretion of HBsAg and HBeAg, reduced HBV total RNA and pregenomic RNA levels, and exerted antiviral effects by modulating the extracellular signal-regulated MAP kinases (ERK1/2)-hepatocyte nuclear factor 4 alpha (HNF4α) axis. Concurrently, the reduction in serum HBV DNA copy number in infected mice confirmed the therapeutic efficacy of Bet against HBV infection *in vivo*. **Conclusion:** These results demonstrate that Bet exhibits anti-HBV activity, which could inform new drug development strategies for HBV.

Keywords: hepatitis B virus (HBV); betulonic acid; extracellular signal-regulated MAP kinases (ERK1/2); hepatocyte nuclear factor 4 alpha (HNF4α)

1. Introduction

Globally, the World Health Organization reports approximately 1.1 million new hepatitis B virus (HBV) infections and around 900,000 related deaths annually [1]. Despite extensive research, identifying specific and effective therapeutic targets and agents for HBV remains a major challenge. Current evidence suggests that HBV initially attaches to HSPGs (Heparan Sulfate Proteoglycans) at the hepatocyte surface with low affinity, followed by specific interaction with NTCP (Sodium Taurocholate Cotransporting Polypeptide) to facilitate internalization [2], followed by viral replication and transcription. Monitoring HBsAg levels is a key indicator of treatment efficacy [3]. Currently, available therapies include interferon-based and nucleoside analogue treatments. However, nucleoside analogues are associated with risks of viral relapse risks [4] and drug resistance development [5]. Interferon therapy, known for its immunomodulatory effects, can induce HBsAg clearance [6], and seroconversion [7]. For instance, a fusion protein combining anti-PD-L1 with an HBV vaccine has shown the potential to eliminate HBsAg in mice [8]. Nevertheless, the current options for achieving a functional cure for HBV are limited [9].

Traditional Chinese medicine (TCM) offers a vast and diverse pool of bioactive compounds, resembling a natural drug library with significant potential for disease treatment and drug development. Betulonic acid (Bet), a pentacyclic triterpenoid compound derived from *Liquidambar formosana* Hance fruit (Hamamelidaceae), was first recorded in the Supplement to the Compendium of Materia Medica (Ben Cao Gang Mu Shi Yi). The Chinese Materia Medica (Zhong Hua Ben Cao) documents the hepatoprotective properties of *Liquidambar formosana*, and modern studies have exhibited that Bet exhibits significant anti-hepatotoxic activity. Additionally, pharmacological studies have demonstrated that Bet and related triterpenoids exert anti-cancer, anti-inflammatory [10,11], and antiviral effects [12,13]. For instance, in treating porcine reproductive and respiratory syndrome (PRRS), Bet can inhibit PRRS virus replication by downregulating cellular ATP [13]. Additionally, Bet has also been discovered to have potential as a therapeutic agent against coronaviruses, owing to its effect on

Copyright: © 2026 The Author(s). Published by IMR Press.
This is an open access article under the CC BY 4.0 license.

Publisher's Note: IMR Press stays neutral with regard to jurisdictional claims in published maps and institutional affiliations.

nonstructural protein 15 (nsp15) [14]. Its acetylene derivatives also exhibit potent anti-inflammatory and hepatoprotective properties [15]. However, the antiviral effect of Bet against HBV has not yet been clearly defined.

Several hepatocyte-specific nuclear factors, including hepatocyte nuclear factors (HNFs), retinoid X receptor, farnesoid X receptor, and peroxisome proliferator-activated receptors, are involved in HBV transcription [16,17]. HNF4α plays a central role in binding to multiple enhancer regions and the pre-core promoter of the HBV genome, thereby regulating viral replication and gene expression. Prior studies have demonstrated that ERK pathway activation effectively downregulates HNF4α and HNF1α expression, which in turn inhibits HBV replication and transcription [18,19,20,21,22,23,24]. Additionally, peroxisome proliferator-activated receptor-γ coactivator 1α (PGC-1α) interacts with HNF4α, Peroxisome proliferator-activated receptor alpha (PPARα), and Peroxisome proliferator-activated receptor gamma (PPARγ), playing a crucial role in supporting HBV replication [25,26,27,28,29]. Nuclear factor NF-kappa-B p65 subunit (NF-κB/p65) can strongly activate the miR-130a promoter, elevating miR-130a expression and thereby suppressing PGC-1α and PPARγ to inhibit HBV replication [30]. Furthermore, p65 may inhibit viral replication by modulating the activity of transcription factor Nuclear receptor subfamily 2 group F member 1 (NR2F1) activity or through direct binding to the HBV core promoter [31,32,33]. The Phosphatidylinositol 4-phosphate 3-kinase (PI3K)/RAC-alpha serine/threonine-protein kinase (AKT)/Serine/threonine-protein kinase mTOR (mTOR) pathway's role in HBV replication is controversial. While some studies report that inhibition of this pathway suppresses HBV replication, others suggest that its activation can also reduce HBV replication, an outcome likely dependent on the specific therapeutic context [18,34,35,36].

In this study, we demonstrate that Bet effectively suppresses HBV replication and transcription *in vitro* and *in vivo*. Mechanistic investigations revealed that Bet activates the Mitogen-activated protein kinase (MAPK) and NF-κB pathways while downregulating the PI3K/AKT/mTOR cascade. This activity reduces the expression levels of HNF1α and HNF4α, two transcription factors essential for HBV replication. However, only inhibition of ERK1/2 effectively reversed the suppression of HBV replication induced by Bet. These findings identify Bet as a novel candidate for therapeutic intervention against HBV infection.

2. Methods and Materials

2.1 Cell Culture and Drugs

Human hepatoma cell lines HepG2.2.15 (CC-Y1583, EK-Bioscience, Shanghai, China) and Huh-7 (Cat. TCH-C217, Haixing Biosciences) cells were cultured in DMEM medium (KGM12800-500, KEeyGEN Bio TECH) supplemented with 10% fetal bovine serum (FBS, A5256701, Gibco) at 37 °C under 5% CO_2. Cells were routinely monitored, and passaging was performed approximately every 48 h upon reaching 70%–80% confluence. To maintain HBV genome stability, periodic G418 (350 μg/mL) selection was performed. Cell lines were validated by STR profiling and tested negative for mycoplasma. Cells were passaged and maintained for no more than 10 passages.

For screening, a validated L6730-Anti-Virus TCM monomer library (containing 270 purified compounds, HPLC purity ≥98%) was commercially sourced from TOPSCIENCE. Betulonic acid (B823662, 50 mg, MACKLIN) was dissolved in dimethyl sulfoxide (DMSO) at a stock concentration of 10 mM, stored at –80 °C, and diluted in culture medium immediately before use. Vehicle controls (DMSO ≤0.1%) were included in all experiments to eliminate solvent effects.

2.2 CCK-8 Assay

HepG2.2.15 cells were seeded in 96-well plates at a density of 10,000 cells/well and cultured for 24 h to reach approximately 70% confluency. The cells were then treated with specified concentrations of test compounds (antiviral TCM monomer or Bet). After 48 h of incubation at 37 °C and 5% CO_2, cell proliferation was quantified using a CCK-8 assay kit (40203ES80, Yeasen, Shanghai) according to the protocol of the manufacturer. Absorbance was measured at 450 nm using a microplate reader (800TS-SN, Agilent Technologies). Each sample was analyzed in triplicate.

2.3 Flow Cytometry Assay

HepG2.2.15 cells were seeded in a 6-well plate at a density of 500,000 cells/well. Upon reaching approximately 70% confluence, the medium was aspirated and replaced with fresh medium containing 10 or 20 μM Bet for the experimental groups, 0.1% (v/v) DMSO for the vehicle control, or drug-free complete medium for the blank control. Following a 48-hour incubation, the cells were harvested by gentle trypsinization and centrifuged at 1500 rpm for 5 min. The pellet was carefully resuspended in 200 μL of ice-cold phosphate-buffered saline (PBS, KGL2206-500, KeyGEN). For viability assessment, 2 μL of propidium iodide (PI) solution (40710ES03, Yeasen, 1 mg/mL stock) was added to achieve a final concentration of 10 μg/mL, and the suspension was mixed gently and incubated for 15 min at 4 °C in the dark. Cell viability was analyzed using a NovoCyte Flow Cytometer (NovoCyte 2060R, Agilent Technologies). Events were first gated on a forward scatter area (FSC-A) versus side scatter area (SSC-A) plot to exclude debris and retain the main cellular population. Doublets were excluded by plotting FSC-A versus FSC-H (or FSC-W), and only singlet events along the diagonal were retained.

2.4 Enzyme-linked Immunosorbent Assay (ELISA)

HepG2.2.15 cells were seeded in a 6-well plate at a density of 500,000 cells/well. Upon reaching approxi-

mately 70% confluence, the cells were treated for 48 h with Bet (10 or 20 μM), Entecavir monohydrate (ETV) (HY-13623A, MCE, 20 μM), RG-7834 (HY-117650A, MCE, 20 μM) or 0.1% (v/v) DMSO as a control. This treatment protocol was also applied to p1.3 × HBV-transfected Huh-7 cells. After treatment, the cell culture supernatants were collected and centrifuged at 3000 rpm for 5 min to remove cellular debris. HBsAg and HBeAg expression in the clarified supernatants were quantified using commercial ELISA Kits (HBsAg ELISA kit, Lot: 2024040408; HBeAg ELISA Kit, Lot: E202310023-2; Zhongshan Biotechnology). For mouse serum samples, the levels of aspartate aminotransferase (AST) and alanine transaminase (ALT) were determined using commercial mouse AST ELISA kit (ml058659, mlbio) and mouse ALT ELISA kit (ml058648, mlbio) according to the manufacturer's instructions. Finally, absorbance was measured at 450 nm using a calibrated microplate reader (800TS-SN, Agilent Technologies), with 630 nm used as a reference wavelength when necessary.

2.5 RNA Extraction and cDNA Synthesis

After treatment with 0.1% (v/v) DMSO, Bet (10 or 20 μM), ETV (20 μM) or RG-7834 (20 μM), total RNA was isolated from HepG2.2.15 cells or p1.3 × HBV-transfected Huh-7 cells using TRIzol reagent (15596026CN, Invitrogen) according to the protocol of the manufacturer. RNA purity and concentration were verified using NanoDrop spectrophotometry (NanoDrop OneC, Thermo Fisher). First-strand cDNA was synthesized immediately using the Novoprotein Reverse Transcription System (E047-01A, Novoprotein).

2.6 Real-time Quantitative reverse transcription PCR (RT-qPCR)

RT-qPCR was performed using NovoStart® SYBR qPCR SuperMix Plus (E096-01A, Novoprotein) to quantify the expression levels of HBV total RNA and pregenomic RNA (pgRNA). GAPDH was used as the endogenous reference gene for normalization, and relative RNA expression changes were calculated using the $2^{-\Delta\Delta Ct}$ method. All experiments were performed in triplicate.

All primer sequences utilized in the current study are presented in the following:

pgRNA-For TCTTGCCTTACTTTTGGAAG,
pgRNA-Rev AGTTCTTCTTCTAGGGGACC,
total RNA-For ACGTCCTTTGTTTACGTCCCGT,
total RNA-Rev CCCAACTCCTCCCAGTCCTTAA,
GAPDH-For GGTGAAGGTCGGTGTGAACG,
GAPDH-Rev CTCGCTCCTGGAAGATGGTG.

2.7 Western Blot Assay

After the drug treatment cycle, the mice were sacrificed and their liver tissues were removed. Freshly isolated mouse liver tissues were immediately homogenized in RIPA lysis buffer containing 1 × protease inhibitor cocktail using a grinder. Lysates were centrifuged at 12,000 rpm for 15 min at 4 °C, and supernatants were collected.

For Bet-treated HepG2.2.15 cells and p1.3 × HBV-transfected Huh-7 cells, cells were washed three times with ice-cold PBS, then lysed in identical RIPA buffer with inhibitors on ice (40–60 min, vortexing every 10 min) followed by centrifugation (12,000 rpm, 15 min, at 4 °C) to harvest supernatants. Protein concentration was determined by using the BCA assay (P0010, Beyotime). After denaturation of the protein by boiling it at 100 °C for 10 min, 10 μg of each sample was separated by SDS-PAGE (8–12% gradient gels, PG112, Yatase) and then transferred to Immun-Blot® PVDF membranes (ISEQ0010, Millipore) via wet transfer (100 V for 60 min). Following transfer, the membranes were blocked with 5% (w/v) skimmed milk for 2 h, then incubated overnight at 4 °C with the corresponding primary antibody. After three times 10-min TBST washes, membranes were probed with horseradish peroxidase (HRP)-conjugated secondary antibodies (1:8000 dilution, 2 h, room temperature (RT)). Protein signals were detected using Clarity™ Western ECL substrate (Bio-Rad) and Densitometric analysis of Western blot bands was performed using ImageJ (Fiji 2, https://imagej.net/imagej-wiki-static/Welcome) software. The relative expression levels of target proteins were quantified by normalizing to the internal reference protein (Actin).

Western blot primary antibodies included anti-β-actin (Sc-47778, Santa Cruz), Anti-PPARγ Mouse mAb (Sc-7273, Santa Cruz), Anti- PGC1α Rabbit mAb (ET1702-96, HUABIO), Anti-HNF1α Mouse mAb (Sc-393925, Santa Cruz), Anti-HNF4α Mouse mAb (Sc-374229, Santa Cruz), HBsAg Rabbit mAb (NB100-62652, NOVUS), p38 (5A1) Mouse mAb (200782, Chengdu Zen-bioscience Co., Ltd.), Phospho-p38 MAPK (Thr180/Tyr182) (9211S, CST), ERK1/2 Rabbit mAb (R22685, Chengdu Zen-bioscience Co., Ltd.), Phospho-p44/42 MAPK (Erk1/2) Rabbit mAb (4370S, CST), MEK Rabbit mAb (ET-1602-3, HUABIO), Phospho-MEK Rabbit mAb (ET-1609-50, HUABIO), JNK Rabbit mAb (R24778, ZENBIO), Phospho-JNK Rabbit mAb (4778S, CST), mTOR Rabbit mAb (2972S, CST), Phospho-mTOR Rabbit mAb (2971S, CST), AKT Rabbit mAb (R23412, Chengdu Zen-bioscience Co. Ltd.), Phospho-AKT (Thr308) Rabbit mAb (341790, CST), PI3K Rabbit mAb (4257S, CST), Phospho-PI3K Rabbit mAb (H65150018, HUABIO), NF-κB P65 Rabbit mAb (R25149, Chengdu Zen-bioscience Co., Ltd.), Phospho-NF-κB P65 Rabbit mAb (3033S, CST), IκBα Rabbit mAb (R380682, ZENBIO), Phospho- IκBα(Ser32) (14D4) Rabbit mAb (2859S, CST). Secondary antibodies included Goat anti-Rabbit IgG (H+L) secondary antibody, HRP (65-6120, Invitrogen) and Goat anti-Mouse IgG (H+L) Secondary Antibody, HRP (31431, Invitrogen).

2.8 Southern Blot

p1.3 × HBV-transfected Huh-7 cells were treated with Bet for 48 h. After being washed with PBS, HBV DNA was extracted using a DNA extraction kit (B0813B, TIANGEN) according to the manufacturer's protocol. Following DNA quantification, agarose gel electrophoresis was carried out using a 1% agarose gel at 140 V until the loading buffer migrated out of the gel, and the band positions were visualized under ultraviolet light.

The gel was subjected to depurination in 0.25 M HCl twice for 5 min each, then equilibrated in 0.4 M NaOH three times for 15 min each, and further equilibrated in 20 × SSC transfer buffer for 5 min. Downward capillary transfer was then conducted. The transfer stack was assembled from bottom to top in the order: absorbent paper, filter paper, nylon membrane (FFN10, Beyotime), agarose gel, filter paper, siphon filter paper, and weight. Membrane transfer was performed at room temperature for more than 16 h. The nylon membrane was removed, air-dried, and subjected to UV cross-linking (120 mJ/cm^2, 2 min).

In parallel, the probe was prepared in advance according to the instructions of the Biotin Random Prime DNA Labeling Kit (D3118, Beyotime). The hybridization oven was preheated to 55 °C. The nylon membrane was placed into a hybridization tube, and 10 mL of Quick Hybridization Solution (R0229, Beyotime) supplemented with 200 µL of 50 × Denhardt's solution was added for prehybridization at 55 °C for 3 h. For overnight hybridization, the membrane was incubated with 10 mL of Quick Hybridization Solution containing 200 µL of 50 × Denhardt's solution and the probe at a final concentration of 25 ng/mL.

On the next day, the nylon membrane was washed three times with washing buffer at room temperature for 5 min each, followed by a 15 min wash at 42 °C. Chemiluminescent detection was performed following the manufacturer's instructions of the Chemiluminescent Biotin-labeled Nucleic Acid Detection Kit (D3308, Beyotime). Finally, the membrane was exposed and visualized using a chemiluminescence imaging system (Touch Imager XLi Lot: AGX2312Y02, e-BLOT Life Science (Shanghai) Co., Ltd.).

2.9 Inhibitors Rescue Experiment

HepG2.2.15 and p1.3 × HBV-transfected Huh-7 cells were seeded in a 6-well plate. Upon reaching approximately 60% confluence, the cells were treated with or without the following inhibitors/agonists: ERK inhibitor SCH772984 (942183-80-4, MACKLIN), 5 µM, AKT agonist SC79 (T2274, TargetMol), 10 µM, NF-κB inhibitor SC75741 (HY-10496, MCE), 5 µM, and p38 inhibitor Adezmapimod hydrochloride (HY-10256A, MCE), 10 µM. After a 12-h pretreatment, each group was subdivided into drug-treated and control subgroup, receiving either 20 µM Bet or 0.1% (v/v) DMSO. The cells were then co-treated with the corresponding compounds for 48 h. Following this incubation, we analyzed HBsAg levels in the culture supernatant and in cellular RNA and protein.

2.10 RNA Sequencing and Analysis.

HepG2.2.15 cells were seeded in six-well plates at a density of 5 × 10^5 cells/well. After 24 h, the culture medium was replaced with fresh medium containing either 20 µM Bet or 0.1% (v/v) DMSO, control and experimental group cells were collected 48 h after drug treatment and washed with PBS. Total RNA was isolated using TRIzol, and libraries were prepared and quantified on an Illumina NovaSeq 6000 (paired-end 150 bp; Illumina, Inc.) by Azenta Life Science. Differentially expressed transcripts were defined as |log2(fold change) | >1 with $p < 0.05$ and analyzed using iDEP 2.0 (https://bioinformatics.sdstate.edu/idep/) [37]. KEGG pathway enrichment analysis of DEGs using clusterProfiler (v4.0.5).

2.11 AAV HBV Mouse Model

Animal experiments were approved by the Animal Experiment Ethics Committee of Bengbu Medical University (Approval No.: 291 [2024]) and conducted in compliance with the Guide for the Care and Use of Laboratory Animals (8th ed., NRC, 2011), the PRC Regulations for the Administration of Affairs Concerning Experimental Animals, the Ministry of Science and Technology's Guiding Opinions on the Treatment of Laboratory Animals (2006), and GB/T 35892-2018. Mice were kept in animal rooms maintained on 12-h light-dark cycle, temperature and humidity-controlled, between 20–23 °C and 30–70%, respectively. All animals were allowed to acclimatise to the facility for at least 7 days before the start of any experimental procedure, to allow recovery from transportation stress. Health status was monitored daily during the acclimatisation period, and animals showing signs of illness, injury or failure to regain body weight were excluded and not used in the study. The HBV mouse model was established using 6−8-week-old male C57BL/6 mice (GemPharmatech (Nanjing, China)) through tail vein injection of AAV8-HBV1.3 vector (5 × 10^{10} viral vector genome equivalents/-mouse, genotype D/ayw, PackGen Biotech). Model validation was confirmed by quantitative ELISA for serum HBsAg levels (HBsAg ELISA Kit, Lot: 2024040408, Zhongshan Biotechnology) at 14 days post-injection. Successfully infected mice were randomly assigned to receive either Bet (5 mg/kg, 100 µL administered intraperitoneally twice a week) or vehicle control (0.1% DMSO in PBS, administered intraperitoneally twice weekly). Serum samples were collected every 10 days to measure HBsAg levels. Forty days after treatment initiation, the mice were euthanized following institutional animal care guidelines. Mice were anesthetized via intraperitoneal injection of Avertin (1.25% m/v, Cat: MA1612-1, Meilunbio) at a dose of 18 µL/g. Mice were euthanized by CO_2 inhalation. The chamber displacement rate was maintained at 30–70% of its vol-

ume per minute using a CO_2 flow rate of 10–15 L/min at a pressure of 0.1–0.3 MPa. Death was confirmed approximately five minutes later by the absence of a heartbeat and pupillary dilation. Cervical dislocation was performed as a secondary method when death was not assured. Serum samples were collected for HBsAg quantification (ELISA) and HBV DNA copy quantification, which was performed by real-time PCR using the HBV Real-time PCR Test kit (Cat: DA0031, DaAn Gene Co., Ltd.) according to manufacturer's instructions. Liver tissue specimens were obtained for subsequent analyses, including Western blot and immunohistochemical staining. For each experiment, the experimental unit was defined as an individual animal. Animals were allocated to experimental groups using randomized cage assignment, and group assignments were prepared by an investigator who was not involved in outcome assessment. To minimize potential confounding, animals were distributed across treatment groups according to cage location, and experimental procedures were performed in a balanced order whenever feasible. Investigators performing HBsAg ELISA were blinded to group allocation where applicable. Sample labels were coded, and group identities were revealed only after data processing and statistical analysis were completed. For experiments in which full blinding was not possible, the rationale and the steps taken to reduce detection bias were described. Qianqian Xu and Sien Ma were aware of the group allocation at the different stages of the experiment. The sample size for each animal experiment was determined based on a priori power analysis. The primary outcome was HBV inhibition, defined as the change in serum HBV DNA from baseline to the end of treatment, expressed as $\log_{10}$ IU/mL. No a priori power calculation was performed, as reliable variance estimates were unavailable. No statistical method was used to predetermine sample size for exploratory analyses unless otherwise stated. No specific inclusion or exclusion criteria were predefined, and no animals or data points were excluded from the analysis.

2.12 Immunohistochemistry

Fresh liver tissues from control and experimental mice were fixed in 4% paraformaldehyde (PFA) (#P0099; Beyotime) and embedded in paraffin. Paraffin-embedded tissues were sectioned into 3–4 µm slices, followed by deparaffinization in xylene and rehydration through a graded ethanol series (100%, 95% and 70%). Antigen retrieval was performed using a citrate-based retrieval solution. Endogenous peroxidase activity was blocked by incubating sections with 3% hydrogen peroxide for 10 min at room temperature. Non-specific binding sites were blocked with 5% bovine serum albumin (BSA) for 30 min at room temperature. Tissue sections were then incubated with primary antibodies against HBsAg and HBcAg for 60 min at room temperature (or overnight at 4 °C for enhanced sensitivity). After washing, sections were incubated with HRP-conjugated secondary antibodies for 30–60 min at room temperature. Immunoreactivity was visualized using 3,3'-diaminobenzidine as the chromogenic substrate, followed by counterstaining with hematoxylin, dehydration in an ascending alcohol series, and mounting with a permanent medium.

2.13 Luciferase Reporter Gene Assay

1.3 × HBV Luciferase plasmid [38], which contains the HBV Enhancer I, Enhancer II, and core promoter regions (kindly provided by Dr. Hongxia Fan from Tianjin Medical University), was transfected into Huh-7 cells using the KeygenMAX 3000 Transfection Reagent (KGA9705-1.5, KeyGen BioTECH). After 24 h of incubation, cells were treated with 20 µM Bet for 48 h. Promoter activity was quantified by luminescence intensity using a Firefly Luciferase Reporter Assay Kit (#RG005, Beyotime).

2.14 Immunofluorescence

The six-well plate was covered with cover slips, and approximately 500,000 HepG2.2.15 cells were plated per well. After 24 h, the cells were treated with 20 µM Bet. Cells were washed twice with PBS after 48 h, then 500 µL of 4% PFA was added, the cells were fixed at room temperature for 15 min, and washed thrice with PBS. Next, 1 mL of 0.2% Triton X-100 (diluted in PBS: 10 mL of PBS + 20 µL of Triton X-100) was added, incubated at room temperature for 15 min, and washed thrice with PBS. Next, 500 µL of 5% BSA was added to each well and blocked at room temperature for 1 h. After PBS washing, the antibody (Phospho-NF-κB P65 Rabbit mAb (3033S, CST)) was diluted in 1% BSA at 1:200 and incubated overnight. The next day, the samples were washed four times with PBS for 5 min each. The secondary antibody, Goat anti-Rabbit IgG (H+L) Cross-Adsorbed ReadyProbes™ Secondary Antibody, Alexa Fluor™ 594(R37117, Invitrogen) (diluted 1:500), was incubated at room temperature for 1 h and then washed four times with PBS. After staining the nuclei with DAPI diluted 1:1000 in the dark for 15 min, washing them 3 times with PBS, and removing the cover slips, the cover slips were sealed with a fluorescence quencher. The samples were observed with a confocal microscope (Stellaris 5 Leica).

2.15 Statistical Analysis

Experimental data were analyzed using GraphPad Prism 10 (GraphPad Software, Inc.) and ImageJ (Fiji 2, https://imagej.net/imagej-wiki-static/Welcome). Error bars in all graphs denote standard deviation derived from three or more independent biological replicates. Imaging data and immunoblots are representative of at least three independent experiments unless otherwise noted. Each *in vivo* data point corresponds to a mouse from an independent experimental group. The statistical significance of comparisons between the two groups was determined using Stu-

dent's *t*-test. The assumptions of the statistical tests were checked before analysis. Normality was evaluated using the Shapiro-Wilk test and normal Q-Q plots, and homogeneity of variance using Levene's test. Data meeting both assumptions were analysed with the *t*-test or one-way ANOVA with Tukey's post-hoc test. Heterogeneous variances were handled using the Welch test with Games-Howell post-hoc comparisons, and non-normal data were transformed (log or square root) or analysed with non-parametric tests (Mann-Whitney U or Kruskal-Wallis with Dunn's test and Bonferroni correction), with results reported as median (IQR). Cohen's d with 95% confidence intervals based on the non-central t distribution was used for two-group comparisons, eta-squared with non-central F-based confidence intervals was used for one-way ANOVA, and partial eta-squared was reported for factorial designs. For longitudinal tumour growth data analysed with linear mixed-effects models, we report the fixed-effect estimates and their 95% confidence intervals. The significance of multiple groups was determined using one-way or two-way ANOVA where appropriate, with significance levels set at $*p < 0.05$, $**p < 0.01$, $***p < 0.001$, and $****p < 0.0001$.

3. Results

3.1 Discovery of Bet as a Potent Anti-HBV Reagent From a TCM Monomer Library

TCM serves as a vast reservoir of bioactive compounds with substantial potential for drug development. Leveraging the recognized multi-target activity and favorable safety profile of TCM, we used the HepG2.2.15 cell line, a well-established *in vitro* HBV replication model, to screen natural compounds with anti-HBV activity from an antiviral TCM monomer library containing 270 natural compounds (L6730, HPLC purity ≥98%). HepG2.2.15 cells were treated with 20 μM of the library compounds for 48 h (Fig. 1A). Cell viability and HBsAg secretion were assessed after a 48-h treatment period using the CCK-8 assay and ELISA, respectively (Fig. 1B,C). Among the tested compounds, Bet, a lupane-type triterpenoid, was prioritized for further investigation because of its potent anti-HBV activity and underexplored therapeutic potential. A dose–response assay (0–40 μM) was performed to determine the optimal working concentration. Bet exhibited low cytotoxicity in the 10–20 μM range (**Supplementary Fig. 1A**), as further confirmed by flow cytometry analysis of cell death and microscopy observation of cell morphology (**Supplementary Fig. 1B–D**). Cells were treated with the same drug concentration for 48 h, Bet was compared with entecavir and RG7834. The effects of the drugs were detected using ELISA and RT-qPCR. The experimental results demonstrated that Bet exhibited superior anti-HBV effect compared to entecavir and RG7834 in suppressing HBsAg and HBeAg secretion (**Supplementary Fig. 1E–H**). ELISA results exhibited that Bet treatment (10 and 20 μM) for 24, 48, and 72 h, reduced the secretion of HBsAg and HBeAg into the culture medium of HepG2.2.15 cells in a dose-dependent manner (Fig. 1D,E) and time-dependent manner (Fig. 1F,G). Furthermore, Bet treatment (10 and 20 μM) for 24, 48, and 72 h remarkably inhibited the HBV RNA levels, including total RNA and pgRNA, in a dose- and time-dependent manner (Fig. 1H–K). Collectively, these findings suggest that Bet inhibits HBV replication.

3.2 RNA-seq Analysis Identifies the Mechanism of Bet -Mediated Inhibition of HBV Replication

To elucidate the molecular mechanisms underlying Bet-mediated anti-HBV activity, we conducted Bulk RNA sequencing of HepG2.2.15 cells treated with Bet or without. In summary, HepG2.2.15 cells were seeded into six-well platesat a density of 5×10^5 cells per well and treated with Bet at 0 and 20 μM for 48 h. Cells were collected, and TRIzol was used to extract RNA for RNA-seq analysis. Under stringent criteria ($|\log_2 FC| \geq 1$, Q-value ≤ 0.05), 4222 differentially expressed genes (DEGs) were identified, including 1534 upregulated and 2688 downregulated genes (Fig. 2A). Hierarchical clustering revealed distinct transcriptional profiles between Bet-treated and control groups (Fig. 2B). RT-qPCR validation of 20 DEGs (10 upregulated and 10 downregulated) exhibited strong consistency with RNA-seq data (**Supplementary Fig. 2A,B**).

KEGG pathway analysis revealed multiple enriched signaling pathways among DEGs (Fig. 2C). Although PPAR and AMPK pathways were not among the most statistically significant, their biological relevance to HBV regulation has been well-supported by previous studies. For instance, microRNA-130a suppresses viral replication by co-targeting PGC1α and PPARγ [30]. HALLMARK pathway analysis further highlighted NF-κB signaling as the most significantly enriched (FDR <0.05; Fig. 2D). TF.Target.RegNetwork analysis exhibited that HBV-relevant transcription factors, such as HNF4α, HNF1α, and PPARγ, target genes were significantly downregulated (Fig. 2E). Protein-protein interaction (PPI) analysis using the STRING database identified functional links between HNF4α and PGC1α (**Supplementary Fig. 2C,D**), suggesting that Bet may modulate a coordinated transcriptional network.

These results indicate that Bet inhibits HBV by targeting key signaling pathways (PPAR, AMPK, and NF-κB) and transcriptional regulators (HNF4α, PGC1α, and PPARγ), disrupting viral transcription and replication.

3.3 Bet Regulates PI3K/AKT/mTOR, NF-κB, and MAPK Pathways and Inhibits Key HBV-related Transcription Factors

Based on transcriptome analysis, we hypothesized that Bet exerts its antiviral effects by modulating transcription-factor networks and key signaling pathways. HepG2.2.15 cells were treated with Bet (10 and 20 μM) for 48 h, and

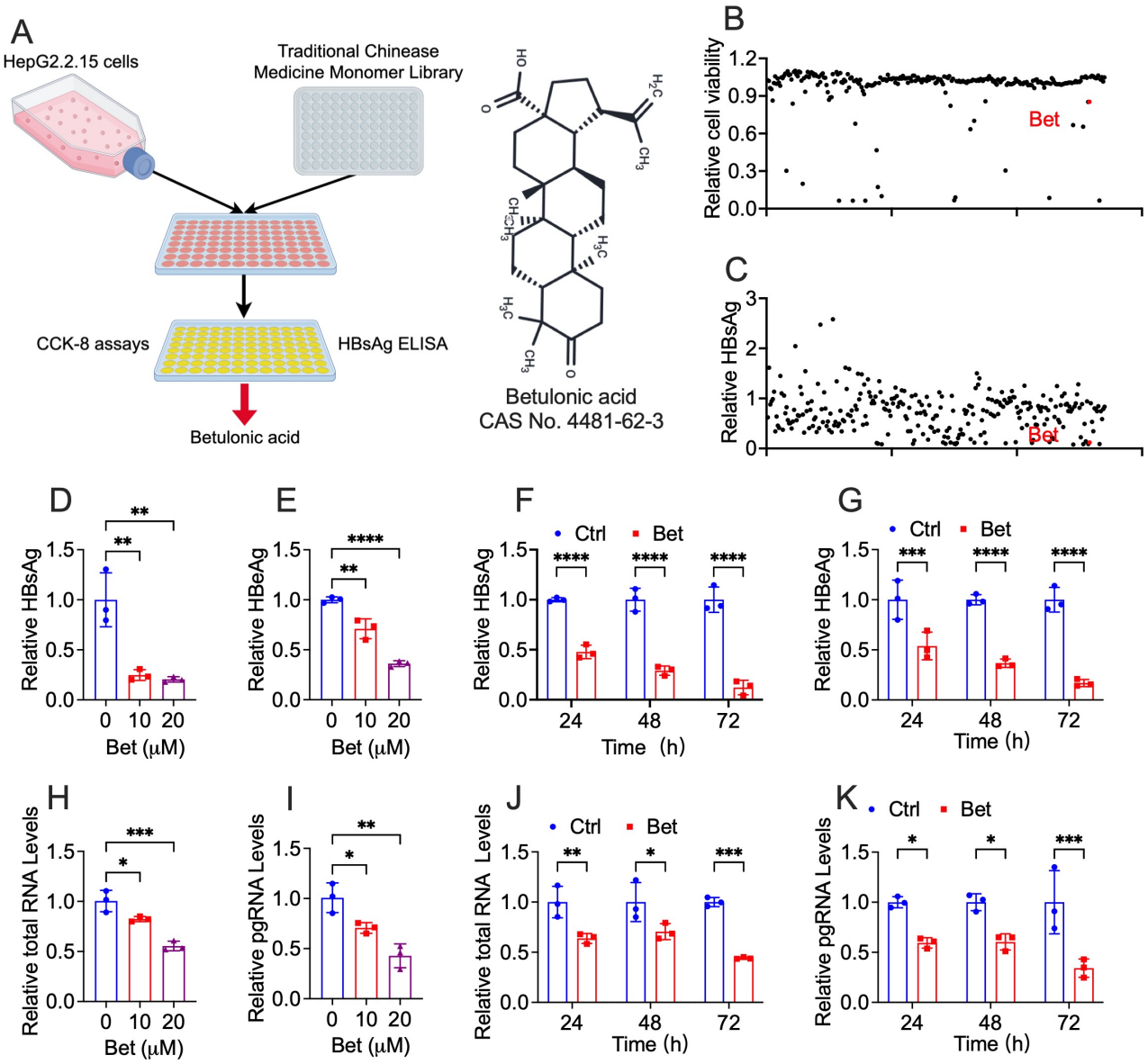


Fig. 1. Discovery of Bet as a potent anti-HBV agent from a TCM monomer library. (A) Schematic of the screening workflow for HBV-inhibiting monomeric compounds using HepG2.2.15 cells through CCK-8 and ELISA assays. Created by FigDraw2.0, ID: WWIIOae222 (https://www.figdraw.com/static/index.html#/). (B) The CCK-8 assay was used to determine the cytotoxicity of 270 TCM compounds in HepG2.2.15 cells after 48 h of treatment. (C) Detecting HBsAg in HepG2.2.15 cells treated with 270 TCM compounds for 48 h using ELISA. (D,E) Secretion levels of HBsAg and HBeAg in the supernatant of HepG2.2.15 cells following a 48 h culture in medium containing Bet (0, 10, and 20 μM). (F,G) Secretion levels of HBsAg and HBeAg after Bet (20 μM) treatment of HepG2.2.15 for 24, 48 h, and 72 h were evaluated using ELISA. (H,I) HepG2.2.15 cells were cultured in medium containing Bet (0, 10, and 20 μM) for 48 h, after which RT-qPCR quantified intracellular HBV RNA expression. (J,K) HBV RNA expression after Bet (20 μM) treatment of HepG2.2.15 for 24, 48, and 72 h was evaluated using RT-qPCR. Data analysis was performed using two-way ANOVA. *$p < 0.05$, **$p < 0.01$, ***$p < 0.001$, and ****$p < 0.0001$. HBV, hepatitis B virus; TCM, traditional Chinese medicine; RT-qPCR, Real-time Quantitative reverse transcription PCR.

the cells were then collected for Western blot. The results suggested that Bet significantly downregulated HBV-related transcription factors (PGC1α, HNF4α, HNF1α, and PPARγ) in a dose-dependent manner and reduced HBsAg levels (Fig. 3A). Studies have demonstrated that HNF4α is a key transcription factor for the HBV core promoter and enhancer. It can directly bind to these critical regions and strongly drive pgRNA synthesis, a prerequisite for viral replication. Furthermore, several agents have been reported to block viral replication by downregulating or degrading

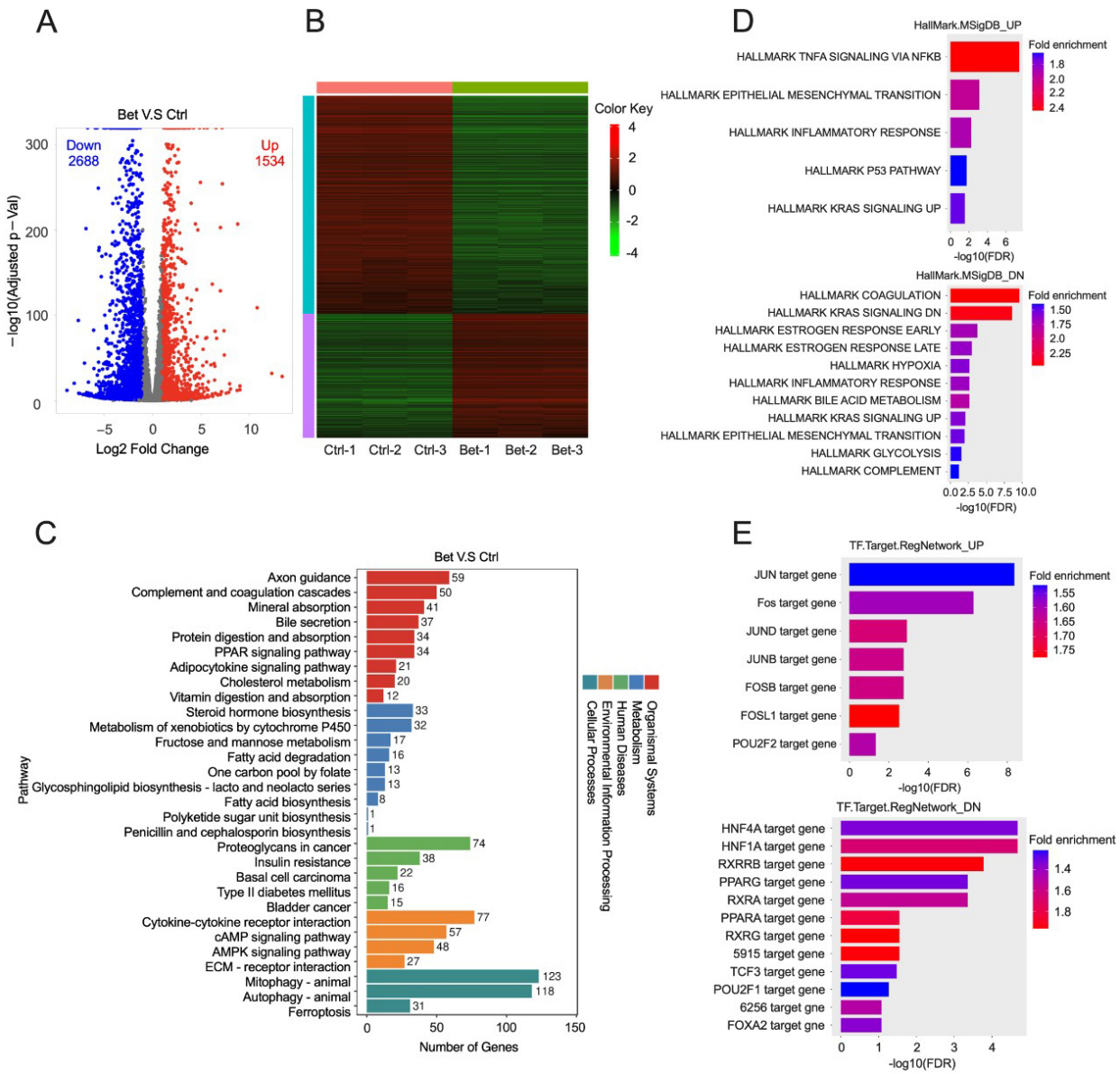


Fig. 2. RNA-seq analysis identifies the mechanism of Bet -mediated inhibition of HBV replication. (A) Volcano plot identifies 4222 DEGs from a comparison between HepG2.2.15 cells treated with Bet for 48 h and DMSO group, filtered by $|\log_2 FC| \geq 1$ and Q ≤ 0.05 (DESeq2). Among them, 1534 were upregulated (red) and 2688 were downregulated (blue). (B) Hierarchical clustering heatmap (Z-score normalized, Euclidean distance) exhibiting complete segregation of Bet-treated (n = 3) from the control (n = 3) groups. (C) KEGG pathway enrichment analysis of DEGs using clusterProfiler (v4.0.5). The top 30 significantly enriched pathways (hypergeometric test, FDR ≤ 0.05) were ranked by enrichment score. (D) The HALLMARK gene set enrichment analysis (GSEA) was performed using the MSigDB database (v7.5.1). (E) Transcription factor network analysis using RegNetwork (v2.0).

HNF4α [16,39,40]. Consequently, targeting HNF4α is an effective strategy for inhibiting covalently closed circular DNA (cccDNA) transcription in HBV infection. Previous research also indicated that the MAPK/ERK pathway plays an important role in inhibiting HBV replication. Activation of ERK1/2 inhibits HBV replication through downregulation of HNF4α [19,20,41,42,43]. We found that Bet treatment increased the phosphorylation of MEK, ERK1/2, and p38 (Fig. 3B).

Furthermore, previous studies have suggested that inhibition of the PI3K/AKT/mTOR pathway contributes to suppression of HBV replication and related liver cancer progression [44]. We found that Bet treatment slightly reduced the phosphorylation of PI3K, AKT, and mTOR in a dose-dependent manner (Fig. 3C). Moreover, previous studies suggested that the NF-κB pathway is involved in the regulation of HBV replication.

We found that Bet treatment resulted in a significant reduction in total IκBα and a more pronounced decrease in

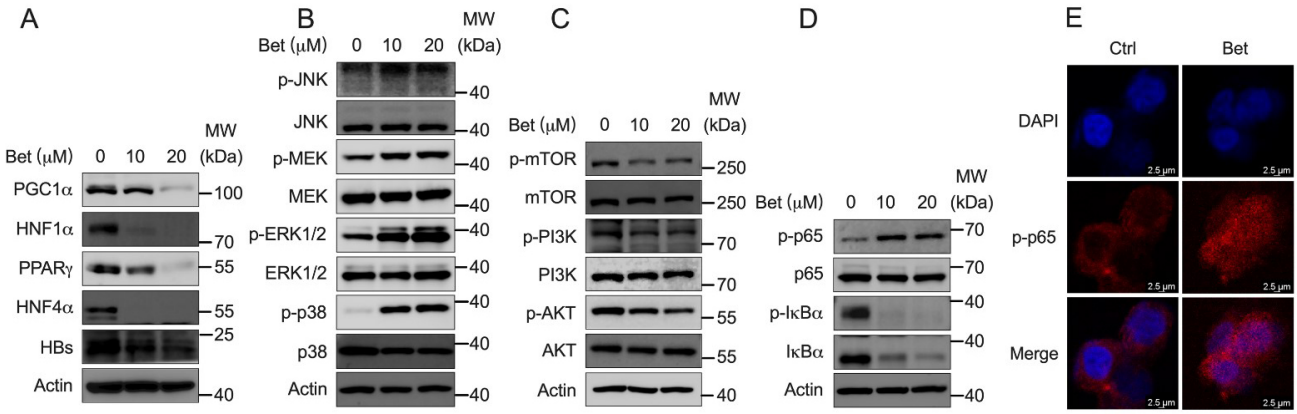


Fig. 3. Bet regulates PI3K/AKT/mTOR, NF-κB, and MAPK pathways and inhibits key HBV-related transcription factors. (A) Western blot detectedthe expression of HBV-related transcription factors PGC1α, HNF4α, HNF1α, PPARγ, and HBsAg. (B) Western blot analysis shows dose-dependent upregulation of the expression of MAPK pathway components including p38, JNK, MEK, and ERK1/2. (C) Western blot analysis shows dose-dependent downregulation of PI3K/AKT/mTOR pathway. (D) Western blot analysis shows that Bet activates p65 and inhibits IκBα phosphorylation in HepG2.2.15 cells. (E) Immunofluorescence analysis of p-p65 localization in HepG2.2.15 cells (scale bar: 2.5 μm).

phosphorylated IκBα (p-IκBα) (Fig. 3D). This observation can be explained by the marked promotion of IκBα phosphorylation and subsequent degradation. The robust decrease in total IκBα and near disappearance of p-IκBα do not indicate the absence of pathway activation; instead, they likely reflect highly efficient and rapid negative feedback following NF-κB activation. Concurrently, IκBα degradation leads to the release and phosphorylation of p65. Consistently, an increase in phosphorylated p65 (p-p65) was observed, which was further confirmed by immunofluorescence exhibiting nuclear translocation of p-p65 (Fig. 3E), a hallmark of NF-κB activation. Elevated p-p65 levels further verified that the downstream effects of NF-κB signaling were initiated.

All Western blot results were subjected to densitometric analysis to verify the protein expression changes induced by Bet treatment (**Supplementary Fig. 3**). These data collectively indicate that Bet inhibits HBV replication by suppressing PGC1α and HNF4α, which may regulate MAPK/ERK, PI3K/AKT/mTOR, and NF-κB pathways.

3.4 Bet Inhibits HBV Replication in 1.3 × HBV Transfected Huh-7 Cells

To validate the anti-HBV effects of Bet in another cellular context, Huh-7 cells were transfected with a 1.3 × HBV plasmid. Following treatment with Bet (20 μM), secretion of HBsAg and HBeAg was reduced (Fig. 4A,B), along with HBV RNA levels (Fig. 4C,D). A luciferase assay using the 1.3 × HBV-Luc plasmid further confirmed reduced viral transcription (Fig. 4E).

Western blot analysis of Huh-7 cells confirmed the downregulation of HBsAg and key transcription factors (PGC1α, PPARγ, HNF4α, and HNF1α) (Fig. 4F). Furthermore, Bet (20 μM) inhibited the phosphorylation of PI3K, AKT, and mTOR (Fig. 4G) and activated the ERK/MEK, JNK, and p38 pathways (Fig. 4H). The increase in p-p65 expression observed in HepG2.2.15 cells was also seen in Huh-7 cells (Fig. 4I). Furthermore, Southern blot analysis revealed that Bet treatment decreased the level of HBV relaxed circular DNA (rcDNA), indicating the inhibition of HBV replication (Fig. 4J).

Additionally, densitometric and statistical analyses of Western blot confirmed the significant differences in protein expression (**Supplementary Fig. 4**). These findings confirm that Bet exerts potent antiviral activity in HepG2.2.15 and Huh-7 cell models, indicating its anti-HBV efficacy *in vitro*.

3.5 ERK1/2 was Required for Bet–Mediated Inhibition of HBV Replication via HNF4α

We investigated which signaling pathway was essential for Bet-induced inhibition of HBV replication. HepG2.2.15 cells were treated with Bet in combination with ERK1/2 inhibitor (SCH772984), AKT agonist (SC79), p38 inhibitor (Adezmapimod hydrochloride) or NF-κB inhibitor (SC75741). After treatment for 48 h, HBsAg secretion was detected using ELISA, and HBV RNA levels were evaluated by RT-qPCR. The results indicated that the ERK1/2 inhibitor partially reversed Bet-mediated inhibition of HBV replication (Fig. 5A–C), whereas the AKT agonist, p38 inhibitor, and NF-κB inhibitor did not (**Supplementary Fig. 5**). HepG2.2.15 cells were treated with Bet, with or without an ERK1/2 inhibitor, for 48 h, then collected and subjected to Western blot analysis. The results exhibited that the ERK1/2 inhibitor effectively reduced ERK1/2 phosphorylation and significantly attenuated Bet-mediated inhibition of HNF4α and HBsAg levels (Fig. 5G).

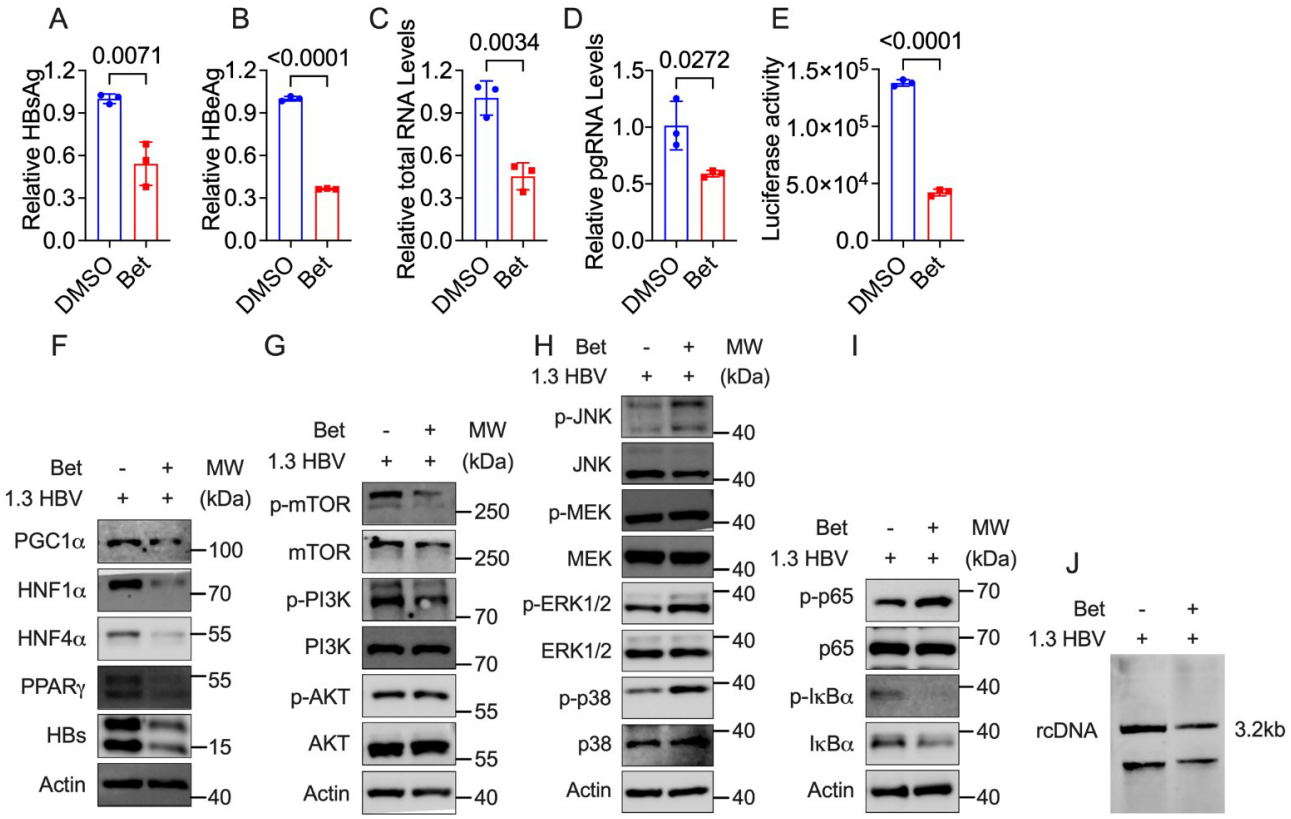


Fig. 4. Bet inhibits HBV replication in 1.3 × HBV-transfected Huh-7 cells. (A,B) HBsAg and HBeAg expression were inhibited in the medium after treatment with Bet in HBV-transfected Huh-7 cells. (C,D) The expression levels of total RNA and pgRNA were reduced in Huh-7 cells transfected with HBV under Bet. (E) Luciferase levels increased after Luc plasmid transfection in Huh-7 cells and decreased after drug treatment. (F) Bet inhibits the expression of HBV-related transcription factors. (G) Western blot indicated that Bet inhibited phosphorylation of PI3K/AKT/mTOR. (H) Western blot analysis revealed that Bet upregulated the expression of MAPK pathway components, including p38 pathway, and JNK, MEK, and ERK1/2, in Huh-7 cells. (I) Bet activates p65 and inhibits phosphorylation of IκBα when it acts on HBV-transfected Huh-7 cells. (J) Southern blot analysis displayed that Bet treatment decreased the level of relaxed circular DNA (rcDNA) in Huh-7 cells transiently transfected with 1.3 × HBV plasmid. Data were analyzed using Student's *t*-tests for specific comparisons.

To further validate that ERK1/2 activation is required for Bet-mediated inhibition of HBV replication, Huh-7 cells were transiently transfected with HBV 1.3 copy plasmid and treated with Bet in combination with the ERK1/2 inhibitor for 48 h. ELISA (Fig. 5D) and RT-qPCR (Fig. 5E,F) results displayed that while Bet retained partial antiviral activity in inhibitor-treated cells, its inhibitory effect on HBV replication was significantly weakened compared to treatment without the inhibitor. Western blot indicated that an ERK1/2 inhibitor remarkably reversed Bet-mediated inhibition of HNF4α and HBsAg levels in HBV 1.3 copy plasmid-transfected Huh-7 cells (Fig. 5H), densitometric and statistical analyses of Western blot confirmed the significant differences in protein expression (**Supplementary Fig. 6**).

Overall, Bet-mediated inhibition of HBV replication is dependent on the ERK1/2-HNF4α axis.

3.6 Bet Demonstrates Antiviral Efficacy in an HBV Mouse Model

To assess the *in vivo* efficacy of Bet, a HBV mouse model was established using C57BL/6 mice by intravenously injected with AAV8-1.3HBV (Fig. 6A). Bet treatment reduced serum HBsAg and HBV DNA levels (Fig. 6B,C) and also reduced serum ALT and AST levels (Fig. 6D,E). Immunohistochemistry revealed a marked decrease in HBV-positive hepatocytes following Bet treatment (Fig. 6F), and Western blot analysis confirmed reduced hepatic HBsAg and HNF4α expression (Fig. 6G).

These results demonstrate that Bet exerts strong anti-HBV activity *in vivo* and highlight its potential as a promising candidate for the novel anti-HBV therapeutics.

4. Discussion

HBV, a small enveloped DNA virus belonging to the *Hepadnaviridae* family, possesses a 3.2 kb partially double-

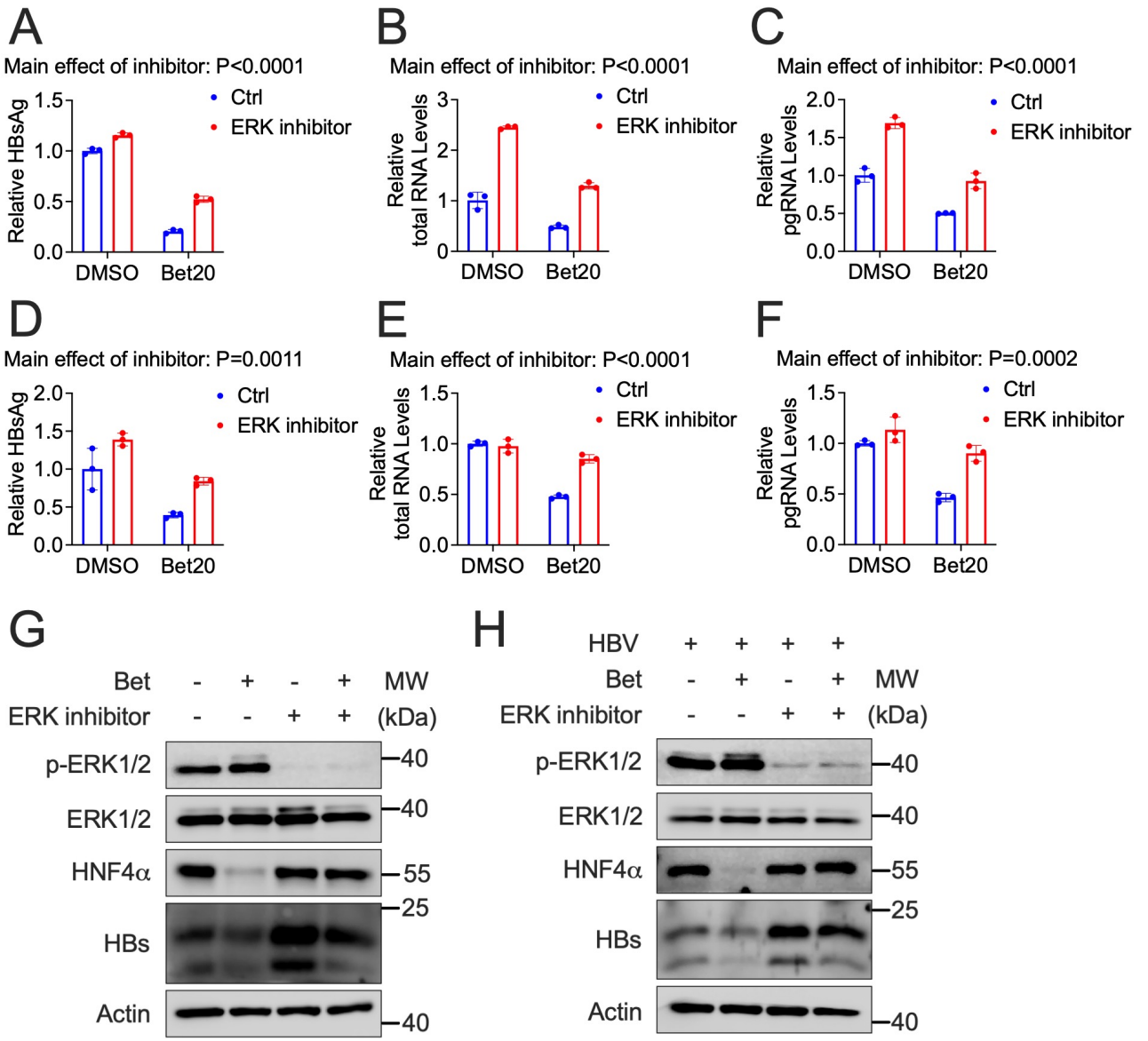


Fig. 5. ERK1/2 was required for Bet-mediated inhibition of HBV replication via HNF4α. (A) The ERK1/2 inhibitor partially reverses Bet-mediated inhibition of HBsAg. (B,C) Following ERK1/2 inhibitor treatment, the suppressive effect of Bet on total RNA and pgRNA levels in HepG2.2.15 cells was partially attenuated. (D) Bet-mediated suppression of HBsAg expression in the culture medium of HBV-transfected Huh-7 cells was attenuated upon treatment with an ERK1/2 inhibitor. (E,F) Under ERK1/2 inhibitor treatment, the suppressive effect of Bet on total RNA and pgRNA levels in Huh-7 cells transfected with HBV was reversed. (G,H) The ERK1/2 inhibitor elevated the protein levels of HBs and HNF4α in HepG2.2.15 and HBV-transfected Huh-7 cells, partially counteracting the inhibitory effects of Bet. Data analysis was performed using two-way ANOVA.

stranded DNA genome. Upon infection, this genome is converted into covalently closed cccDNA minichromosomes within hepatocyte nuclei [45,46]. HBV cccDNA serves as the transcriptional template for the 3.5 kb pgRNA, precore RNA, 2.4 kb preS1 RNA, 2.1 kb preS2/S RNA, and the 0.7 kb HBx RNA. These transcripts function as templates for the translation of polymerase (P), surface proteins (S; preS1, preS2, and S), precore/core (C), and HBx proteins [47,48]. By screening a TCM compound library, we identified Bet as a potential anti-HBV agent. *In vitro*, Bet effectively reduced HBsAg and HBeAg secretion, decreased HBV pgRNA and total RNA levels, and inhibited HBV promoter activity. Using a novel AAV/HBV mouse model, we further confirmed that Bet treatment significantly lowered serum HBsAg and HBV DNA levels and suppressed hepatic expression of HBsAg and HBcAg. This study reveals the previously unreported anti-HBV activity of Bet.

RNA-seq and pathway enrichment analyses of Bet-treated HepG2.2.15 cells revealed significant upregula-

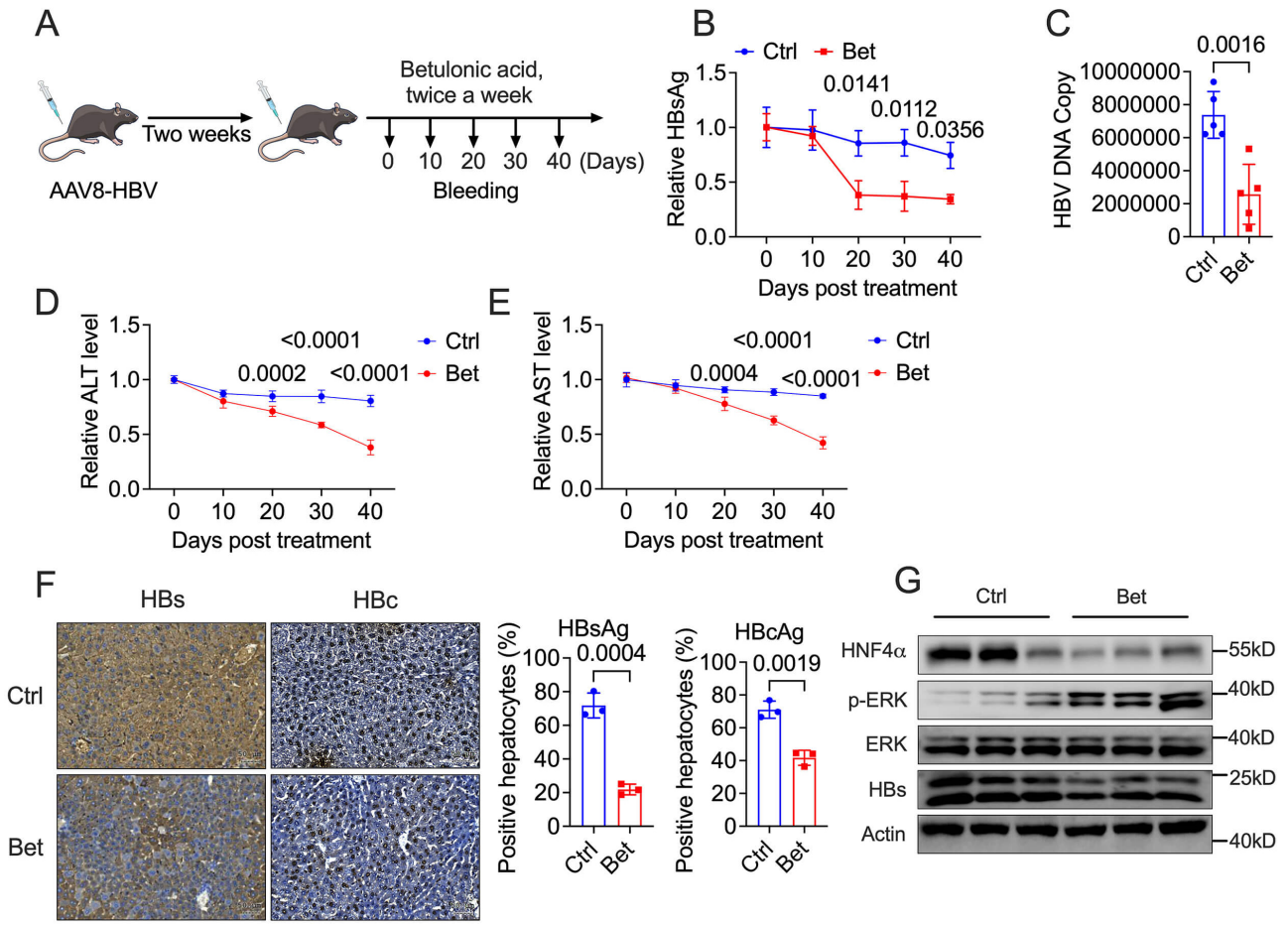


Fig. 6. Bet demonstrates antiviral efficacy in an HBV mouse model. (A) HBV replication was established in male C57BL/6 mice (n = 5/group) by tail vein injection of AAV8-HBV1.3. Bet (5 mg/kg) or vehicle control was administered intraperitoneally twice a week from day10 to day40. Serial bleedings were performed every 10 days to monitor HBsAg. (B) Serum HBsAg levels in mice were measured every 10 days during intraperitoneal Bet injection. (C) RT-qPCR (copies/mL) was used to detect the HBV DNA load in the serum of mice after 40 days of Bet treatment. (D) Relative serum ALT levels in mice were measured every 10 days during intraperitoneal Bet injection. (E) Relative serum AST levels in mice were measured every 10 days during intraperitoneal Bet injection. (F) Hepatocellular HBcAg and HBsAg expression were analyzed by using immunohistochemistry (scale bar: 50 μm). (G) Liver HBsAg, HNF4α, ERK1/2 and p-ERK1/2 protein levels were assessed by Western blot (β-actin as loading control). All data are presented as mean ± SEM. Data were analyzed using a two-way ANOVA or Student's *t*-tests for specific comparisons.

tion of NF-κB pathway-related genes and downregulation of *HNF4α*, *HNF1α*, and *PPARγ* compared to control cells. Western blot analysis corroborated these findings, exhibiting increased p-p65 levels and decreased expression of HNF4α, HNF1α, and PPARγ. Previous studies have demonstrated that HNF4α and HNF1α bind to the HBV Enhancer I and II regions to promote HBV transcription [22] and that HNF4α also activates HNF1α by binding to its promoter [17]. It is well established that ERK1/2 activation suppresses HBV replication by downregulating HNF4α expression [18,19,20,21,22,49]. In our study, Bet treatment significantly activated MAPK signaling, as evidenced by the phosphorylation of MEK, ERK1/2, p38, and JNK. Consequently, Bet may inhibit HBV transcription through the p-ERK/HNF4α axis. The roles of JNK and p38 activation in HBV replication have been contradictory in previous studies [41,50,51,52,53,54]. In this study, we found that the ERK1/2 inhibitor (SCH772984) significantly reversed Bet-mediated inhibition of HBV replication, whereas the p38 inhibitor (Adezmapimod hydrochloride) did not, suggesting that Bet may suppress HBV replication by modulating ERK1/2-HNF4α axis.

The NF-κB signaling pathway also plays a critical role in HBV infection. p-p65 directly binds to the HBV core promoter, thereby inhibiting transcription and replication. Additionally, p-p65 indirectly restricts HBV replication by modulating interferon pathways and other transcription factors [32,33,55,56,57]. In this study, we found that Bet enhanced p65 phosphorylation and promoted its nuclear translocation. However, NF-κB inhibitor (SC75741)

could not reverse Bet-mediated inhibition of HBV replication, which should be further investigated in the future. The PI3K/AKT/mTOR pathway and autophagy are also known to regulate HBV replication, although previous findings have been inconsistent [34]. Our data exhibited that Bet slightly inhibited phosphorylation of PI3K, AKT, and mTOR. However, AKT agonist (SC79) could not reverse Bet-induced inhibition of HBV replication. Additionally, we did not evaluate whether Bet affects autophagy, which is tightly regulated by the AKT/mTOR pathway and plays a critical role in HBV restriction. This warrants further investigation.

5. Limitations

In the mechanistic study of the anti-HBV effect of betulonic acid, we identified ERK as the primary signaling pathway involved. Meanwhile, changes in other signaling pathways were also observed. Although the crosstalk and regulatory relationships among these pathways were not further investigated in the present study, the potential interactions between different signaling pathways deserve consideration in future research. In addition, as is well known, long-term inhibition of the HBV-related transcription factor HNF4α may lead to adverse effects [58,59]. As a master switch of hepatic metabolism, sustained suppression of HNF4α disrupts the differentiation status and metabolic functions of hepatocytes [60]. The therapeutic intervention in mice was maintained only for a relatively short period; we have not yet determined whether long-term Bet administration would eventually result in liver injury or other adverse effects on the host. Further studies are warranted to clarify whether sustained HNF4α inhibition is required for Bet to exert long-term anti-HBV activity. Given the critical role of cccDNA in HBV replication, even though our findings have verified the anti-HBV activity of Bet, we acknowledge that the absence of direct quantification or assessment of cccDNA constitutes one of the limitations of this study.

6. Conclusion

We identified Bet as a novel anti-HBV compound that inhibits HBV transcription and replication *in vitro* and *in vivo*. Mechanistically, Bet suppresses HBV replication mainly through activation of the ERK signaling pathway, and may simultaneously exert effects on other signaling pathways, thereby reducing HNF4α expression. Collectively, our study provides new evidence supporting the potential application of Bet in the clinical treatment of chronic HBV infection.

Availability of Data and Materials

Most of the data in this study are presented in the figures and tables of the manuscript. For the sequencing data, only processed results are included in the present article. We clearly state in the manuscript that all processed and relevant raw data are available from the corresponding authors upon reasonable request, in compliance with the journal's requirements.

Author Contributions

All authors contributed to the study conception and design. BZ, QQX, SEM and MMD conceptualized and designed the study; QQX, SEM, YP, SML, YTZ, LLW, JWC and YRL performed the experiments and data analysis; QQX, SEM, MMD and BZ wrote the manuscript. YP and YRL revised the manuscript. All authors have read and agreed to the published version of the manuscript. The authors declare that all data were generated in-house, that no paper mill was used and that no AI tool has been used for the generation of text or figures. All authors contributed to editorial changes in the manuscript. All authors have participated sufficiently in the work and agreed to be accountable for all aspects of the work.

Ethics Approval and Consent to Participate

Animal experiments were approved by the Animal Experiment Ethics Committee of Bengbu Medical University (Approval No.: 291 [2024]) and cand lists the specific regulations applied: the Guide for the Care and Use of Laboratory Animals (8th ed., NRC, 2011), the PRC Regulations for the Administration of Affairs Concerning Experimental Animals, the Ministry of Science and Technology's Guiding Opinions on the Treatment of Laboratory Animals (2006), and GB/T 35892-2018. The study was carried out in accordance with internationally recognized standards for the care and management of laboratory animals, including the ARRIVE guidelines (Animal Research: Reporting of *In Vivo* Experiments) and 3R principle: substitution, reduction, and optimization.

Acknowledgment

Thanks to all the peer reviewers for their opinions and suggestions.

Funding

This work was supported by National Natural Science Foundation of China (82372786, 82572976), the Anhui Province University Outstanding/Excellent Youth Research Project (2023AH020049 and 2023AH030089), the Research Start-up Funding (2023KYQD010) of Institute of Health and Medicine, Hefei Comprehensive National Science Center.

Conflicts of Interest

The authors declare no conflicts of interest.

Supplementary Material

Supplementary material associated with this article can be found, in the online version, at https://doi.org/10.31083/IJP50778.

References

[1] World Health Organization. Global hepatitis report 2026. World Health Organization: Geneva. 2026.

[2] Quirino A, Marascio N, Branda F, Ciccozzi A, Romano C, Locci C, et al. Viral Hepatitis: Host Immune Interaction, Pathogenesis and New Therapeutic Strategies. Pathogens (Basel, Switzerland). 2024; 13: 766. https://doi.org/10.3390/pathogens13090766

[3] European Association for the Study of the Liver. EASL clinical practice guidelines on the management of hepatitis B virus infection. Journal of Hepatology. 2025; 83: 502–583. https://doi.org/10.1016/j.jhep.2025.03.018

[4] Lai CL, Wong DKH, Wong GTY, Seto WK, Fung J, Yuen MF. Rebound of HBV DNA after cessation of nucleos/tide analogues in chronic hepatitis B patients with undetectable covalently closed. JHEP Reports : Innovation in Hepatology. 2020; 2: 100112. https://doi.org/10.1016/j.jhepr.2020.100112

[5] Liao H, Zhang H, Shao J, Li X, Zheng WV, Li L, et al. Nucleos(t)ide analogues altered quasispecies composition of hepatitis B virus (HBV)-resistant mutations in serum HBV DNA and serum HBV RNA. Journal of Medical Virology. 2023; 95: e28612. https://doi.org/10.1002/jmv.28612

[6] Zhao Q, Liu H, Tang L, Wang F, Tolufashe G, Chang J, et al. Mechanism of interferon alpha therapy for chronic hepatitis B and potential approaches to improve its therapeutic efficacy. Antiviral Research. 2024; 221: 105782. https://doi.org/10.1016/j.antiviral.2023.105782

[7] Wang Y, Guo L, Shi J, Li J, Wen Y, Gu G, et al. Interferon stimulated immune profile changes in a humanized mouse model of HBV infection. Nature Communications. 2023; 14: 7393. https://doi.org/10.1038/s41467-023-43078-5

[8] Meng CY, Sun S, Liang Y, Xu H, Zhang C, Zhang M, et al. Engineered anti-PDL1 with IFNα targets both immunoinhibitory and activating signals in the liver to break HBV immune tolerance. Gut. 2023; 72: 1544–1554. https://doi.org/10.1136/gutjnl-2022-327059

[9] Choi HSJ, Tonthat A, Janssen HLA, Terrault NA. Aiming for Functional Cure With Established and Novel Therapies for Chronic Hepatitis B. Hepatology Communications. 2022; 6: 935–949. https://doi.org/10.1002/hep4.1875

[10] Lombrea A, Scurtu AD, Avram S, Pavel IZ, Turks M, Lugiņina J, et al. Anticancer Potential of Betulonic Acid Derivatives. International Journal of Molecular Sciences. 2021; 22: 3676. https://doi.org/10.3390/ijms22073676

[11] Shao L, Yan Y, Wang N, Tan Q, Huang Y, Lei L, et al. Betulonic acid regulates oviduct epithelial cell inflammation through the TLR4, MAPK, and JAK/STAT signalling pathways. Reproduction, Fertility, and Development. 2023; 35: 480–491. https://doi.org/10.1071/RD21380

[12] Liu M, Wang J, Wan X, Li B, Guan M, Ning X, et al. Discovery and structural optimization of 3-O-β-Chacotriosyl betulonic acid saponins as potent fusion inhibitors of Omicron virus infections. Bioorganic Chemistry. 2023; 131: 106316. https://doi.org/10.1016/j.bioorg.2022.106316

[13] Long F, Su L, Zhang M, Wang S, Sun Q, Liu J, et al. Betulonic Acid Inhibits Type-2 Porcine Reproductive and Respiratory Syndrome Virus Replication by Downregulating Cellular ATP Production. International Journal of Molecular Sciences. 2024; 25: 10366. https://doi.org/10.3390/ijms251910366

[14] Stevaert A, Krasniqi B, Van Loy B, Nguyen T, Thomas J, Vandeput J, et al. Betulonic Acid Derivatives Interfering with Human Coronavirus 229E Replication via the nsp15 Endoribonuclease. Journal of Medicinal Chemistry. 2021; 64: 5632–5644. https://doi.org/10.1021/acs.jmedchem.0c02124

[15] Vasilevsky SF, Govdi AI, Shults EE, Shakirov MM, Sorokina IV, Tolstikova TG, et al. Efficient synthesis of the first betulonic acid-acetylene hybrids and their hepatoprotective and anti-inflammatory activity. Bioorganic & Medicinal Chemistry. 2009; 17: 5164–5169. https://doi.org/10.1016/j.bmc.2009.05.059

[16] Teng Y, Xu Z, Zhao K, Zhong Y, Wang J, Zhao L, et al. Novel function of SART1 in HNF4α transcriptional regulation contributes to its antiviral role during HBV infection. Journal of Hepatology. 2021; 75: 1072–1082. https://doi.org/10.1016/j.jhep.2021.06.038

[17] Xia C, Tang W, Geng P, Zhu H, Zhou W, Huang H, et al. Baicalin down-regulating hepatitis B virus transcription depends on the liver-specific HNF4α-HNF1α axis. Toxicology and Applied Pharmacology. 2020; 403: 115131. https://doi.org/10.1016/j.taap.2020.115131

[18] Yu Y, Hu H, Zhang Y, Zhang Z, Ying S, Dong S, et al. Hedyotis chrysotricha aqueous extract inhibits hepatitis B surface antigen and viral replication via hepatocyte nuclear factor 4α regulation. Phytomedicine : International Journal of Phytotherapy and Phytopharmacology. 2025; 143: 156726. https://doi.org/10.1016/j.phymed.2025.156726

[19] Dai XQ, Cai WT, Wu X, Chen Y, Han FM. Protocatechuic acid inhibits hepatitis B virus replication by activating ERK1/2 pathway and down-regulating HNF4α and HNF1α in vitro. Life Sciences. 2017; 180: 68–74. https://doi.org/10.1016/j.lfs.2017.05.015

[20] Xie M, Guo H, Lou G, Yao J, Liu Y, Sun Y, et al. Neddylation inhibitor MLN4924 has anti-HBV activity via modulating the ERK-HNF1α-C/EBPα-HNF4α axis. Journal of Cellular and Molecular Medicine. 2021; 25: 840–854. https://doi.org/10.1111/jcmm.16137

[21] Lou B, Ma G, Yu X, Lv F, Xu F, Sun C, et al. Deubiquitinase OTUD5 promotes hepatitis B virus replication by removing K48-linked ubiquitination of HBV core/precore and upregulates HNF4α expressions by inhibiting the ERK1/2/mitogen-activated protein kinase pathway. Cellular and Molecular Life Sciences : CMLS. 2023; 80: 336. https://doi.org/10.1007/s00018-023-04995-2

[22] Dezhbord M, Kim SH, Park S, Lee DR, Kim N, Won J, et al. Novel role of MHC class II transactivator in hepatitis B virus replication and viral counteraction. Clinical and Molecular Hepatology. 2024; 30: 539–560. https://doi.org/10.3350/cmh.2024.0060

[23] Thongsri P, Pewkliang Y, Borwornpinyo S, Wongkajornsilp A, Ruenraroengsak P, Anurathapan U, et al. Panduratin A from Boesenbergia rotunda suppresses hepatitis B virus by targeting HNF1α and synergizing with antiviral agents. Chinese Medicine. 2026; 21: 10. https://doi.org/10.1186/s13020-025-01285-w

[24] Tong H, Zhang J, Jiang L, Qu R, Lu T, Hu J. Antiviral activity of HuaganJiedu decoction (HGJDD) against hepatitis B virus (HBV) through FOXO4/ERK/HNF4α signal pathway. Journal of Ethnopharmacology. 2025; 340: 119238. https://doi.org/10.1016/j.jep.2024.119238

[25] Shlomai A, Paran N, Shaul Y. PGC-1alpha controls hepatitis B virus through nutritional signals. Proceedings of the National Academy of Sciences of the United States of America. 2006; 103: 16003–16008. https://doi.org/10.1073/pnas.0607837103

[26] Shi Y, Li Y, Huang C, Ying L, Xue J, Wu H, et al. Resveratrol enhances HBV replication through activating Sirt1-PGC-1α-PPARα pathway. Scientific Reports. 2016; 6: 24744. https:

//doi.org/10.1038/srep24744
[27] Tang X, Yan L, Li H, Du L, Shi Y, Huang F, et al. Increased expression of phosphoenolpyruvate carboxykinase cytoplasmic isoform by hepatitis B virus X protein affects hepatitis B virus replication. Journal of Medical Virology. 2019; 91: 258–264. https://doi.org/10.1002/jmv.25300
[28] Yang Y, Ge F, Luo C, Chen Y, Deng J, Yang Y, et al. Inhibition of hepatitis B virus through PPAR-JAK/STAT pathway modulation by electroacupuncture and tenofovir disoproxil fumarate combination therapy. International Immunopharmacology. 2024; 143: 113304. https://doi.org/10.1016/j.intimp.2024.113304
[29] Shen Z, Wu J, Gao Z, Zhang S, Chen J, He J, et al. High mobility group AT-hook 1 (HMGA1) is an important positive regulator of hepatitis B virus (HBV) that is reciprocally upregulated by HBV X protein. Nucleic Acids Research. 2022; 50: 2157–2171. https://doi.org/10.1093/nar/gkac070
[30] Huang JY, Chou SF, Lee JW, Chen HL, Chen CM, Tao MH, et al. MicroRNA-130a can inhibit hepatitis B virus replication via targeting PGC1α and PPARγ. RNA (New York, N.Y.). 2015; 21: 385–400. https://doi.org/10.1261/rna.048744.114
[31] Xie Z, Shen S, Huang K, Wang W, Liu Z, Zhang H, et al. Mitochondrial HIGD1A inhibits hepatitis B virus transcription and replication through the cellular PNKD-NF-κB-NR2F1 nexus. Journal of Medical Virology. 2023; 95: e28749. https://doi.org/10.1002/jmv.28749
[32] Lin YC, Hsu EC, Ting LP. Repression of hepatitis B viral gene expression by transcription factor nuclear factor-kappaB. Cellular Microbiology. 2009; 11: 645–660. https://doi.org/10.1111/j.1462-5822.2008.01280.x
[33] Tian X, Dong H, Lai X, Ou G, Cao J, Shi J, et al. TRIM56 impairs HBV infection and replication by inhibiting HBV core promoter activity. Antiviral Research. 2022; 207: 105406. https://doi.org/10.1016/j.antiviral.2022.105406
[34] Zhu S, Wen H, Wang W, Chen Y, Han F, Cai W. Anti-hepatitis B virus activity of lithospermic acid, a polyphenol from Salvia miltiorrhiza, in vitro and in vivo by autophagy regulation. Journal of Ethnopharmacology. 2023; 302: 115896. https://doi.org/10.1016/j.jep.2022.115896
[35] Kim J, Kwon H, Kalsoom F, Sajjad MA, Lee HW, Lim JH, et al. Ca2+/Calmodulin-Dependent Protein Kinase II Inhibits Hepatitis B Virus Replication from cccDNA via AMPK Activation and AKT/mTOR Suppression. Microorganisms. 2022; 10: 498. https://doi.org/10.3390/microorganisms10030498
[36] Yu J, Shen Z, Chen S, Liu H, Du Z, Mao R, et al. Inhibition of HBV replication by EVA1A via enhancing cellular degradation of HBV components and its potential therapeutic application. Antiviral Research. 2023; 216: 105643. https://doi.org/10.1016/j.antiviral.2023.105643
[37] Ge SX, Son EW, Yao R. iDEP: an integrated web application for differential expression and pathway analysis of RNA-Seq data. BMC Bioinformatics. 2018; 19: 261. https://doi.org/10.1186/s12859-018-2296-7
[38] Doitsh G, Shaul Y. Enhancer I predominance in hepatitis B virus gene expression. Molecular and Cellular Biology. 2004; 24: 1799–1808. https://doi.org/10.1128/MCB.24.4.1799-1808.2004
[39] Yamashita A, Kasai H, Maekawa S, Tanaka T, Akaike Y, Ryo A, et al. Berberine promotes K48-linked polyubiquitination of HNF4α, leading to the inhibition of HBV replication. Antiviral Research. 2024; 232: 106027. https://doi.org/10.1016/j.antiviral.2024.106027
[40] Zhao Z, Hong W, Zeng Z, Wu Y, Hu K, Tian X, et al. Mucroporin-M1 inhibits hepatitis B virus replication by activating the mitogen-activated protein kinase (MAPK) pathway and down-regulating HNF4α in vitro and in vivo. The Journal of Biological Chemistry. 2012; 287: 30181–30190. https://doi.org/10.1074/jbc.M112.370312
[41] Wu L, Wang W, Zhang X, Zhao X, Yu G. Anti-HBV activity and mechanism of marine-derived polyguluronate sulfate (PGS) in vitro. Carbohydrate Polymers. 2016; 143: 139–148. https://doi.org/10.1016/j.carbpol.2016.01.065
[42] Jiang Q, Zhou Z, Du X, Li Y, Guan G, Zhang T, et al. Novel Function of NUP153 in HNF4α Transcriptional Upregulation Contributes to Promoting HBV Replication. Journal of Medical Virology. 2025; 97: e70256. https://doi.org/10.1002/jmv.70256
[43] Li L, Li Y, Xiong Z, Shu W, Yang Y, Guo Z, et al. FoxO4 inhibits HBV core promoter activity through ERK-mediated downregulation of HNF4α. Antiviral Research. 2019; 170: 104568. https://doi.org/10.1016/j.antiviral.2019.104568
[44] Lee J, Kim J, Lee R, Lee E, An HI, Kwon YJ, et al. SOD1 inhibition enhances sorafenib efficacy in HBV-related hepatocellular carcinoma by modulating PI3K/Akt/mTOR pathway and ROS-mediated cell death. Journal of Cellular and Molecular Medicine. 2024; 28: e18533. https://doi.org/10.1111/jcmm.18533
[45] Zhu A, Liao X, Li S, Zhao H, Chen L, Xu M, et al. HBV cccDNA and Its Potential as a Therapeutic Target. Journal of Clinical and Translational Hepatology. 2019; 7: 258–262. https://doi.org/10.14218/JCTH.2018.00054
[46] Deng M, Hou J, Hu J, Wang S, Chen M, Chen L, et al. Hepatitis B virus mRNAs functionally sequester let-7a and enhance hepatocellular carcinoma. Cancer Letters. 2016; 383: 62–72. https://doi.org/10.1016/j.canlet.2016.09.028
[47] Newbold JE, Xin H, Tencza M, Sherman G, Dean J, Bowden S, et al. The covalently closed duplex form of the hepadnavirus genome exists in situ as a heterogeneous population of viral minichromosomes. Journal of Virology. 1995; 69: 3350–3357. https://doi.org/10.1128/JVI.69.6.3350-3357.1995
[48] Jeng WJ, Papatheodoridis GV, Lok ASF. Hepatitis B. Lancet (London, England). 2023; 401: 1039–1052. https://doi.org/10.1016/S0140-6736(22)01468-4
[49] Kim DH, Kang HS, Kim KH. Roles of hepatocyte nuclear factors in hepatitis B virus infection. World Journal of Gastroenterology. 2016; 22: 7017–7029. https://doi.org/10.3748/wjg.v22.i31.7017
[50] Hoppe-Seyler K, Sauer P, Lohrey C, Hoppe-Seyler F. The inhibitors of nucleotide biosynthesis leflunomide, FK778, and mycophenolic acid activate hepatitis B virus replication in vitro. Hepatology (Baltimore, Md.). 2012; 56: 9–16. https://doi.org/10.1002/hep.25602
[51] Bai L, Zhang W, Tan L, Yang H, Ge M, Zhu C, et al. Hepatitis B virus hijacks CTHRC1 to evade host immunity and maintain replication. Journal of Molecular Cell Biology. 2015; 7: 543–556. https://doi.org/10.1093/jmcb/mjv048
[52] Pang J, Zhang G, Lin Y, Xie Z, Liu H, Tang L, et al. Transforming growth factor β-activated kinase 1 transcriptionally suppresses hepatitis B virus replication. Scientific Reports. 2017; 7: 39901. https://doi.org/10.1038/srep39901
[53] Yang Q, Zhang Q, Zhang X, You L, Wang W, Liu W, et al. HoxA10 Facilitates SHP-1-Catalyzed Dephosphorylation of p38 MAPK/STAT3 To Repress Hepatitis B Virus Replication by a Feedback Regulatory Mechanism. Journal of Virology. 2019; 93: e01607–18. https://doi.org/10.1128/JVI.01607-18
[54] Wan H, Ge L, Xiao L, Li J, Wu W, Peng S, et al. 3,4,5-Tri-O-caffeoylquinic acid methyl ester isolated from Lonicera japonica Thunb. Flower buds facilitates hepatitis B virus replication in HepG2.2.15 cells. Food and Chemical Toxicology : an International Journal Published for the British Industrial Biological Research Association. 2020; 138: 111250. https://doi.org/10.1016/j.fct.2020.111250
[55] Xu C, Fan J, Liu D, Tuerdi A, Chen J, Wei Y, et al. Alpha-

kinase 1 (ALPK1) agonist DF-006 demonstrates potent efficacy in mouse and primary human hepatocyte (PHH) models of hepatitis B. Hepatology (Baltimore, Md.). 2023; 77: 275–289. https://doi.org/10.1002/hep.32614

[56] Chen QY, Liu YH, Li JH, Wang ZK, Liu JX, Yuan ZH. DNA-dependent activator of interferon-regulatory factors inhibits hepatitis B virus replication. World Journal of Gastroenterology. 2012; 18: 2850–2858. https://doi.org/10.3748/wjg.v18.i22.2850

[57] Zheng B, Zhang J, Zheng T, Wang H, Li Z, Huan C, et al. ATP1B3 cooperates with BST-2 to promote hepatitis B virus restriction. Journal of Medical Virology. 2020; 92: 201–209. https://doi.org/10.1002/jmv.25599

[58] Park S, Ha YN, Dezhbord M, Lee AR, Park ES, Park YK, et al. Suppression of Hepatocyte Nuclear Factor 4 α by Long-term Infection of Hepatitis B Virus Contributes to Tumor Cell Proliferation. International Journal of Molecular Sciences. 2020; 21: 948. https://doi.org/10.3390/ijms21030948

[59] Van Dender C, Vandewalle J, Libert C. Balancing metabolism and regeneration in liver diseases through HNF4α targeting. Trends in Endocrinology and Metabolism: TEM. 2026; 37: 83–98. https://doi.org/10.1016/j.tem.2025.04.003

[60] Radi SH, Vemuri K, Martinez-Lomeli J, Sladek FM. HNF4α isoforms: the fraternal twin master regulators of liver function. Frontiers in Endocrinology. 2023; 14: 1226173. https://doi.org/10.3389/fendo.2023.1226173